

Pelletization of catalysts supported on activated carbon. A Case Study: clean synthesis of dimethyl carbonate from methanol and CO₂



Preparación de catalizadores de carbón activado estructurados. Un caso de estudio: síntesis limpia de dimetil carbonato a partir de metanol y CO₂

Andrés Felipe Orrego-Romero, Oscar Felipe Arbeláez-Pérez, Felipe Bustamante-Londoño*, Aída Luz Villa Holguín

Grupo de Investigación Catálisis Ambiental, Departamento de Ingeniería Química, Facultad de Ingeniería, Universidad de Antioquia. Calle 70 # 52-21. A. A. 1226. Medellín, Colombia.

ARTICLE INFO

Received May 18, 2015

Accepted October 28, 2015

KEYWORDS

Dimethyl carbonate, pellets, activated carbon, CO₂, Cu-Ni catalysts

Dimetil carbonato, pellets, carbón activado, CO₂, catalizador Cu-Ni

ABSTRACT: The synthesis of Cu-Ni bimetallic catalyst supported on pellets of activated carbon using carboxymethylcellulose (CMC) as a binder is reported. The effect of preparation conditions, such as binder concentration, AC/binder ratio, temperature, and pyrolysis heating rate on the surface area of the pellets, was evaluated. Cu and Ni metals were incorporated on the pellets by conventional incipient wetness impregnation. The support and the synthesized catalysts were characterized using N₂ adsorption, H₂-TPR, XRD and SEM-EDS techniques. The pelletized catalysts were evaluated for the direct synthesis of dimethyl carbonate DMC (case study). An improved catalytic activity (e.g., ca. 20% increase in conversion) in structured pelletized catalyst in comparison to the powdered catalyst was found.

RESUMEN: Se presenta la síntesis del catalizador bimetalico de Cu-Ni soportado en pellets de carbón activado utilizando carboximetilcelulosa (CMC) como agente aglutinante. Se evaluó el efecto de las condiciones de preparación, tales como concentración de CMC, relación de CMC/Carbón activado, temperatura y velocidad de calentamiento en la pirólisis sobre el área la superficial de los pellets sintetizados. La incorporación de los metales (Cu y Ni) en los pellets se efectuó por impregnación húmeda incipiente convencional. El soporte y los catalizadores sintetizados se caracterizaron mediante adsorción de N₂, H₂-TPR, XRD y técnicas de SEM-EDS. Los catalizadores peletizados se evaluaron en la síntesis directa de dimetil carbonato DMC (caso de estudio), mostrando una actividad catalítica mejorada en comparación con el catalizador en polvo.

1. Introduction

As a result of their very-large surface area and strong adsorption capacity, Activated Carbons, AC, are widely used in air and water purification, energy storage, carbon dioxide fixation, and as supports for the preparation of powdered catalysts [1]. In particular, Table 1 [2-16] lists some of the reactions that have been studied with catalysts supported on AC. However, these processes were performed with powdered catalysts. Therefore, despite their good performance scaling-up of these processes is not yet feasible because of the large amount of catalyst that would be required, as well as the significant pressure drop in a

fixed-bed reactor and the concomitant difficulty in handling fine particles. The use of carbon powders processed into pellets (cylindrically-shaped pieces) [17] or monoliths [18], on the other hand, it can reduce the ratio of catalyst mass to reactor volume, as well as the pressure drop in the bed. In addition, formation of hotspots could be prevented. Thence, a pelletized or monolith-based catalytic system would greatly facilitate scaling-up the reactions. However, although monolithic structured AC-based catalysts or adsorbents have been widely used for abatement of pollutant emissions [19-21], there are no reports in the literature on the use of AC-based pelletized catalyst. The pelletizing process consists of mixing activated carbon with a binder (which helps to keep the carbon particles in a compressed state), followed by the addition of an adequate amount of water to form a paste that is subsequently shaped by compression-molding; the final step is the pyrolysis treatment to favor graphitization and removal of excess binder in the resulting material [22].

* Corresponding author: Felipe Bustamante Londoño
 e-mail: felipe.bustamante@udea.edu.co
 ISSN 0120-6230
 e-ISSN 2422-2844



Table 1 Catalytic processes based on catalysts supported on AC

Catalyst	Reaction	Ref.
Ru/AC	Hydrogenolysis of glycerol	[2]
CeO ₂ -Ni/AC	Water gas shift reaction	[3]
Au/AC	Acetylene hydrochlorination	[4]
Pd-Au/ACC*	Synthesis of H ₂ O ₂ from H ₂ and O ₂	[5]
Co/AC, AC-HNO ₃	CO ₂ reforming of CH ₄	[6-7]
Co ₃ O ₄ -CeO ₂ /AC	Preferential oxidation in H ₂ -rich gases	[8]
Cu/AC, Cu-Ni/AC	Dimethyl carbonate synthesis	[9-11]
Co ₃ O ₄ /AC	Ethyl acetate catalytic combustion	[12]
Cu-Ni/AC	Diethyl carbonate synthesis	[13]
Pt-Ru/AC	Hydrogenation/hydrogenolysis of D-glucose	[14]
AC	Hydrogen production via decomposition of methane	[15]
Ni-Mo/AC	Hydrogenation reaction of CO to higher alcohols	[16]

*ACC: Activated carbon cloth

Although it is expected that binder-catalyst interactions should have no significant influence on the activity, selectivity and stability of the catalyst, depending on the binder and/or preparation conditions, there may be a detrimental effect on some textural and morphologic properties of the catalyst, such as surface area, porosity or pore-size distribution. Both organic and inorganic materials have been used as binders in the pelletization of the activated carbon, but organic binders such as phenolic resin, cellulose powder, polyvinyl alcohol [23], polyvinyl acetate [24], ethyl cellulose and carboxy methyl cellulose (CMC) [25], have attracted more attention because of their good binding properties, inertness and similar chemical nature (relative to activated carbon) which facilitates processing the pellets. In order to have strong, resistant, water- and thermally-stable pellets when CMC is used as binder, the preparation conditions, such as binder loading, temperature and heating ramp during pyrolysis, must be carefully selected in order to minimize pore blocking of the activated carbon and maintain properties such as surface area, microporosity or pore-size distribution. The purpose of this work was, therefore, to understand the effect of experimental conditions in the pelletizing process of commercial activated carbon powder with CMC as binder and obtain optimal preparation conditions to yield pellets with mechanical resistance and minimal impact on catalytic activity. In order to accomplish this, the best experimental conditions for preparing pellets were used for synthesizing Cu, Ni and Cu-Ni catalysts, which were evaluated in the clean, direct synthesis of dimethyl carbonate (DMC) from CO₂ and methanol in gas-phase (see reaction (1)).



DMC is an important chemical product used as a methylating agent, intermediate in the production of higher carbonates and oxygenated fuel additive, and the direct synthesis provides an environmentally-friendly alternative to established processes such as the phosgenation of methanol. Furthermore, the direct synthesis of DMC has been reported on different catalysts supported on Activated Carbon, such as Cu/AC [CH₃OH conversion 2.16%] [26], Ni/AC [CH₃OH conversion 1.43%] [26], Cu-Ni/AC [CH₃OH

conversion 6.6%] [10]. Even though higher conversions were reported with other catalysts, namely Ce-Zr oxide/graphene [CH₃OH conversion 58%] [27], as CeO₂ cannot be easily pelletized [28] we chose Cu-Ni/AC for our case study. The experimental results of the pelletized catalyst were compared with the conventional powder Cu-Ni bimetallic catalyst.

2. Experimental

2.1. Preparation of activated carbon pellets and Cu-Ni/AC pellets

Commercial activated charcoal (AC), Merck (90% particle size < 125 μm), was mixed with an ethanolic solution of carboxymethylcellulose (CMC) as binder; different concentrations of the binder were used, namely 10 wt. %, 20 wt. %, and excess of CMC. The solution was stirred and heated softly for 24 h until ethanol evaporation. The remaining solid was wetted with enough water to form a paste, which was pressed in a uniaxial hydraulic system at 1 metric ton for 15 minutes. The compacted carbon was then extruded in cylindrical shape and cut in pellets (ID 3.175 mm x 4 mm). After drying at 80 °C for 12 h, the pellets were pyrolyzed for 1 hour at 375, 500 or 700 °C in flowing N₂ (25 mL/min) using several heating ramps (1, 5, 10 or 20 °C /min). The effect of CMC concentration in the ethanolic solution (wt. %), pyrolysis temperature, heating ramp, and AC/binder ratio (g AC/cm³ ethanolic binder solution) on surface area of resulting pellets was evaluated. Additionally, two resistance tests were performed for the pellets obtained with each AC/binder ratio; the tests consisted in determining the weight loss of the pellets after treatment in an ultrasonic bath (test 1) or rotation procedure (test 2). Pellets were submerged in water in test 1, and in both ammonia solution and water in test 2; details are given below.

Bimetallic Cu-Ni/AC catalysts were prepared by conventional wetness impregnation of pellets obtained under the optimal preparation conditions. The preparation conditions used in this work are based on previously reported work

[13]. $\text{Cu}(\text{NO}_3)_2 \cdot 3\text{H}_2\text{O}$ (Carlo Erba, 99.5%) and $\text{Ni}(\text{NO}_3)_2 \cdot 6\text{H}_2\text{O}$ (Merck, 99%) were used as metal precursors, and the Cu:Ni molar ratio was fixed at 2:1 with a nominal metal oxide (CuO + NiO) loading of 15 wt. %. The Cu:Ni molar ratio and metal loading were selected to yield a Cu-Ni alloy phase according [13, 26]; furthermore, this molar ratio translates into a significant synergistic effect with respect to the monometallic catalysts [10, 26]. After addition of the precursor solution to AC pellets the resulting mixture was rotavapored at 25 rpm and 180 mmHg of vacuum for 3 h, and then the impregnated pellets were dried at 90 °C for 12 h and pyrolyzed by heating in flowing N_2 (25 mL/min) at 0.5 °C/min up to 500 °C; this temperature was held for 2 h. Finally, the solid was heated in flowing 5% H_2/Ar at a rate of 0.5 °C/min to 600 °C, and held at this temperature for 3 h. The catalyst was labeled as Cu-Ni (2:1)/AC. Monometallic samples of Cu and Ni supported also on carbon pellets, labeled as Cu/AC and Ni/AC, respectively, were prepared for comparison purposes. All pellet and catalyst samples were stored in desiccators under inert atmosphere before using them.

2.2. Catalyst characterization

Specific surface areas of powder and pellets of carbon were determined by N_2 adsorption at 77 K in a Micromeritics Autochem II 2920 equipped with a TCD detector, using the single-point method. Samples were pretreated in flowing 30% N_2/He (25 mL/min) at 250 °C for 30 minutes (using a heating ramp of 10 °C/min). Nitrogen adsorption/desorption isotherms (77 K) of the final catalysts were determined using a Micromeritics 2375 BET instrument equipped with a Vacprep 061 degasser. Prior to measurements, samples were degassed for 2 h at 250 °C and 0.15 mbar to ensure a clean and dry surface. The Brunauer-Emmett-Teller (BET) and the Barrett-Joyner-Halenda (BJH) approaches were used to determine the surface area and pore-size distribution, respectively. H_2 -TPR experiments of oxidized catalyst samples were performed in a Micromeritics AutoChem II 2920 apparatus. In order to ensure a free oxygen atmosphere, 50 mg of samples were pretreated at 5 °C/min to 250 °C for 1 h in flowing helium (70 mL/min), and then cooled down to 40 °C. Thereafter, samples were heated to 800 °C using 5% H_2/Ar (70 mL/min) at 8 °C/min. Signals of H_2 consumption were continuously monitored by a thermal conductivity detector (TCD). The crystallinity of synthesized materials was determined by X-ray diffraction (XRD) on a Phillips PW 1740 diffractometer using Cu K α radiation and Ni filter operated at 40 kV and 20 mA at room temperature. The scanning range was $5^\circ \leq 2\theta \leq 70^\circ$ at $2^\circ/\text{min}$. The diffractograms were compared to JCPDS (Joint Committee of Powder Diffraction Standards) data. The crystallite size of mono and bimetallic particles was calculated from the broadening of X-ray diffraction pattern using the Scherrer's Eq. (2)

$$D_{hkl} = \frac{K \lambda}{\beta_{2\theta} \cos \theta_B} \quad (2)$$

Where D_{hkl} is the average crystallite size (nm), $\beta_{2\theta}$ is the broadening of the full width at half maximum (FWHM) of

the main peak (radians), θ_B is the Bragg's angle (degrees), K is the Scherrer's constant (a value of $K=0.94$ for spherical crystals with cubic symmetry [29] was assumed in this work), and λ is the radiation wavelength (nm). This formula is applicable to crystal structures with particle size smaller than 100 nm [30].

SEM images were taken with a JEOL JSM-6490 microscope using an accelerating voltage of 20kV. Elemental analysis was performed by an energy dispersive X-ray spectroscopy (EDS) instrument coupled to the SEM equipment.

Chemical composition (i.e., Cu and Ni content) of the monometallic and bimetallic samples were determined by atomic absorption spectroscopy (AAS) on a Philips PU9200, using Rhodium radiation at 40 kV. Prior to the analysis the sample (0.05 g) was digested in a 3:1 hydrochloric acid - nitric acid solution.

2.3. Catalytic tests

Catalytic tests were performed in a continuous stainless steel (SS) tubular fixed-bed reactor (ID 7 mm) packed with 1.7 g of catalyst. After catalyst loading, the reactor was sealed and purged using Ar. Methanol vapor was introduced into the reactor by a stream of CO_2 flowing through a SS bubbler containing the liquid alcohol at room temperature. Reaction temperature was controlled by a hot-box system that included an electric forced-convection heater to keep both the reactor and the bypass at the same temperature, avoiding possible condensation in the process lines. The proportional pressure control used a pressure sensor with an accuracy of ± 0.1 bar. All experiments were carried out at P_{CO_2} of 10 bar, GHSV of 988 h^{-1} and varying temperature between 70 and 130 °C; in particular, GHSV was selected according to values reported in the literature for the gas-phase reaction with powdered catalysts [31, 32]. Reactants and products were analyzed online by a mass spectrometer QMS Thermostar 200 (Pfeiffer) and the by-products were determined by gas chromatography (GC-Varian Star 3400, equipped with FID detector and a capillary column DB-WAX (length 60 m ID 0.25 mm)).

Catalytic activity of the pellets was determined by methanol conversion and DMC selectivity, Eqs. (3) and (4), respectively.

$$\text{Methanol Conversion (\%)} = \frac{[\text{CH}_3\text{OH}]_{in} - [\text{CH}_3\text{OH}]_{out}}{[\text{CH}_3\text{OH}]_{in}} \times 100 \quad (3)$$

$$\text{DMC Selectivity (\%)} = \frac{[\text{DMC}]}{[\text{DMC}] + [\text{by-products}]} \times 100 \quad (4)$$

3. Results and discussion

3.1. Effect of preparation conditions on pellet's surface area

The approach commonly used in the literature on pelletizing activated carbon to assess the success of the process for

applications as adsorbent, namely the change in surface area of the pellets with respect to the powder, was used in this work as criterion to determine the best preparation conditions. Figure 1 compares the surface area of activated carbon with several binder loadings (prior to pyrolysis) with that of commercial carbon powder without binder. A drastic decrease in the surface area of commercial carbon by adding 10% CMC binder is observed. Besides, surface area decreased by almost the same proportion when the binder loading increased from 10 to 20%. A further increase in CMC concentration, on the other hand, appears to have a much lower impact on surface area.

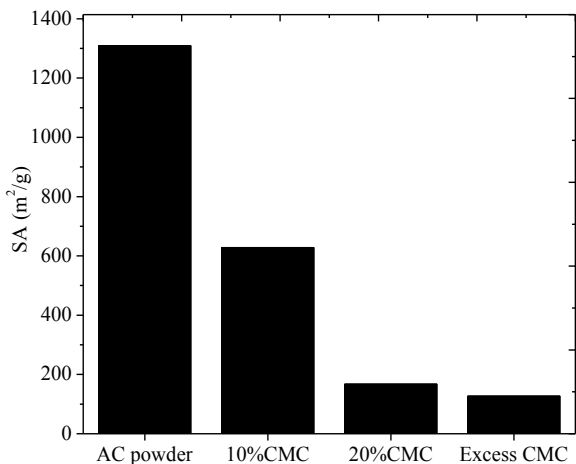


Figure 1 Effect of binder loading on the surface area (SA) of carbon samples before pyrolysis

The net effect of the CMC concentration on the carbon surface area may be further evidenced once the samples are pyrolyzed. Figure 2 shows the surface area of samples in pellets and powder (particle size lower than 125 μm); commercial carbon without binder and pyrolyzed at the same temperature is also shown as comparison.

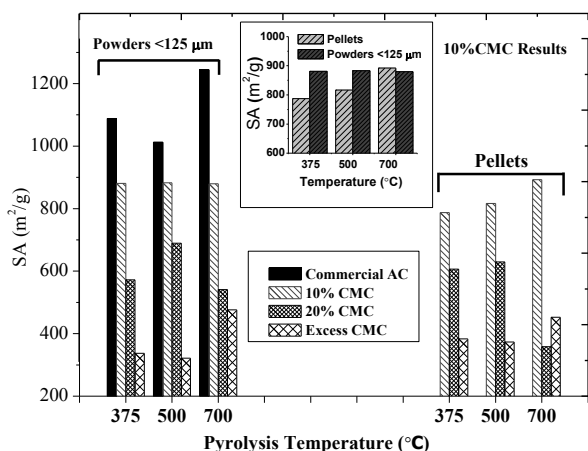


Figure 2 Effect of pyrolysis temperature on the surface area (SA) of carbon pellets and powders (<125 μm) treated with different CMC loadings. The insert compares the effect on SA for both pellets and powders treated with 10% CMC

A decrease in surface area with respect to the commercial carbon without binder was observed for carbon powder with different CMC loadings. At each pyrolysis temperature a reduction in surface area occurs with increasing of CMC loading. The effect of decreasing area occurs for the three pyrolysis temperatures tested where a strong trend of surface area reduction with increasing CMC loading is evidenced. A similar effect is observed with carbon pellets but the surface area values are lower than for powders. On the other hand, TGA-DTG studies [33] revealed that thermal degradation of the CMC occurs between 325 and 350°C. As our pyrolysis temperatures are higher, it is expected a complete decomposition of CMC. Failure to fully recover the initial surface area of the activated carbon, however, may indicate presence of binder residues after pyrolysis treatment, which may block the pores of the carbon, decreasing the surface area even at high pyrolysis temperature. The decrease on surface area is less significant when a binder concentration of 10% in both powder and pellets is used. This is more clearly shown by the insert in Figure 2, which compares the surface area of powders and pellets prepared with 10% CMC loading; whereas the surface area remains almost constant with carbon powders, surface area of the pellets increases with temperature and becomes comparable to powders at 700°C. According to these results, a pyrolysis temperature of 700 °C is considered as an appropriate temperature for treating carbon pellets. Finally, the increase in surface area with pyrolysis temperature observed in some cases may be the result of changes in pore size and pore distribution that would occur at higher temperature of pyrolysis, which, in turn, can affect the surface area of carbon.

The effect of heating rate on the surface area of the pellets was evaluated with a ratio of 15 g AC/200 cm³ ethanolic solution (10 wt.% CMC) and at a pyrolysis temperature of 700 °C, Figure 3. Surface area of all pyrolyzed samples was larger than the surface area of the non-pyrolyzed pellet. In fact, in the non-pyrolyzed pellets the binder would be deposited inside the pores of the carbon, resulting in lower surface area, and, upon pyrolysis the binder is decomposed favoring graphitization and removal of binder from the pores [22]. The percent of deviation from the non-pyrolyzed surface area for the sample heated at 20°C/min was similar to that of the sample heated at 5°C/min. While the pyrolysis temperature is a key factor in the preparation of pellets, the heating rate also plays an important role. In fact, the heat of desorption of the gases produced from the decomposition of CMC (mainly H₂, CO₂, CO, CH₄, C₂H₆, C₂H₄ [33]) should be considered [34, 35], because this complex process involves different types of interactions with the activated carbon (e.g., between -CH₂COO- groups and the surface of carbon layers). Consequently, it can be expected that the higher heating ramp (20°C/min) may favor the decomposition process and, as a result, translate into an increased surface area compared to the ramp of 5°C/min. Therefore, in order to reduce the time of exposure of the carbon to high temperatures, a ramp of 20°C/min was fixed for the pyrolysis treatment.

Once the heating ramp was set, the effect of the amount of binder added to the carbon powders on surface area was evaluated. Specifically, surface areas of pyrolyzed pellets obtained with mixing ratios of 15/200, 25/200 and 50/200 (gAC/mL CMC_(sln)) were determined, Figure 4. The increase

in surface area is more significant as the ratio AC/CMC_(sln) increases. In fact, surface area increases from 453 m₂/g to 900 m₂/g when the AC/CMC_(sln) ratio changes from 15/200 to 50/200. On the other hand, an increase in surface area with respect to non-pyrolyzed pellets was higher with the sample prepared with a ratio of 15/200, whereas the other two samples showed a similar increase with respect to their non-pyrolyzed counterparts.

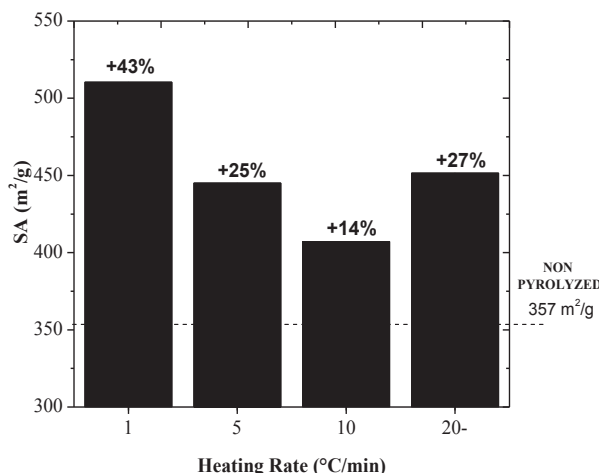


Figure 3 Effect of heating rate of pyrolysis at 700 °C on the surface area of the pellets. Percent on bars indicates the difference on surface area with respect to pellet non-pyrolyzed (357 m²/g)

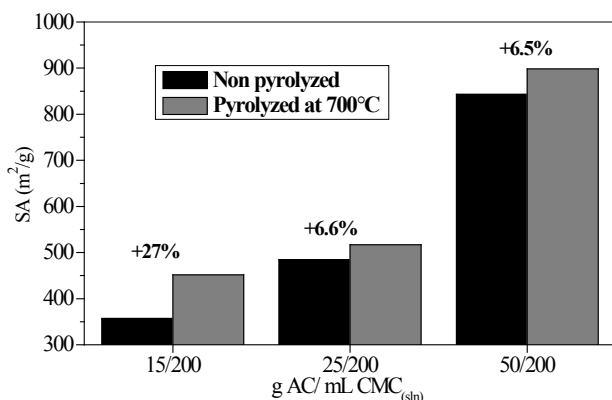


Figure 4 Effect of carbon/binder ratio on the surface area of the pellets. Percent on bars indicates the difference on surface area with respect to non-pyrolyzed pellet

Regarding the surface area of the final material, Figure 4 suggests using the highest AC/CMC_(sln) ratio. However, a loss in consistency was observed when handling such sample; thus, resistance tests on pyrolyzed pellets were performed in order to assess the degree of compaction achieved for each mixture ratio used. These tests consist in determining the weight loss of the pellets after being subjected to vibration in an ultrasonic bath for 90 minutes (test 1) and rotation at 100 rpm and 60 °C for 3 hours in a rotavapor (test 2), Table 2. While a 50/200 mixing ratio favors the surface area of carbon pellets (Figure 4), the results of test 1 show that the consistency of these samples is severely affected, as indicated by the weight loss of 42.3 %, compared to weight losses of 22.5% and 11.8% for the 25/200 and 15/200 ratios, respectively. Results of test 2 show that weight loss with water for 25/200 and 15/200 ratios in the rotation test are almost equal, whilst weight loss with the 50/200 is larger (7.8%). From these results, an AC/CMC_(sln) ratio of 25/200 appears to be an adequate mixing ratio for preparing pellets as suggested by the good degree of compaction and improved mechanical resistance after both vibration and rotation tests. Moreover, the treatment of pellets in H₂O results in a lower weight loss than that observed when the treatment was conducted in an ammonium hydroxide solution.

The comparison between solvents is important since the impregnation of metals over carbon has been conventionally conducted with aqueous ammonia solutions of the salt precursors [36]; our results, on the other hand, indicate the convenience of using water instead of ammonium hydroxide as the dispersion medium of the salt precursors, since it translates into carbon pellets with higher surface area. The AC/binder ratio and the heating rate for the pyrolysis treatment that ensure carbon cylinders that retain its shape without being damaged by handling were established and used to prepare pellets impregnated with Cu and Ni metals.

In summary, the preferred conditions to prepare pellets from activated carbon powders with high surface area using CMC as a binder are: solution of 10% CMC in, carbon-binder ratio of 25 g AC/200 mL CMC_(sln) and pyrolysis at 700 °C with a heating ramp of 20°C/min.

3.2. Catalyst characterization

Catalyst characterization for the bimetallic Cu-Ni (2:1)/AC sample was compared against the monometallic samples. Table 3 summarizes surface areas and metal composition

Table 2 Weight loss of pyrolyzed pellets after vibration in an ultrasonic bath for 90 min (test 1) and rotation in a rotavapor at 100 rpm for 3 h (test 2)

AC/binder ratio (g/mL)	Weight loss [%]		
	Test 1	Test 2 with H ₂ O	Test 2 with ammonia
15/200	11.8	5.5	8.1
25/200	22.5	5.6	9.8
50/200	42.3	7.8	11.4

of fresh catalyst samples. It is observed that metal loading affects the surface area of carbon (surface area is 764 m₂/g prior to impregnation). The AC surface area was reduced between 10 and 19% after impregnation, pyrolysis and activation with hydrogen. The decrease in surface area may be associated with remnants of binder in the catalyst and/or sintering due to the high temperatures of pyrolysis and reduction steps at 500°C and 600°C, respectively.

Table 3 BET surface area and metal loadings of fresh catalyst samples

Sample	Cu/AC	Cu-Ni (2:1)/AC	Ni/AC
SA (m ² /g) ^(a)	523	692	627
%Cu ^(b)	12.9	8.66	-
%Ni ^(b)	-	2.79	9.43

^(a)Surface area for pellets of activated carbon AC = 764 m²/g

^(b)Copper and nickel loadings were determined by atomic absorption spectroscopy (AAS) on a Philips PU9200

Figure 5 shows X-ray diffraction patterns of mono and bimetallic copper-nickel catalysts. XRD for AC support (not shown) exhibited a broad and low intensity peak at 2θ = 23°, associated with activated carbon [11].

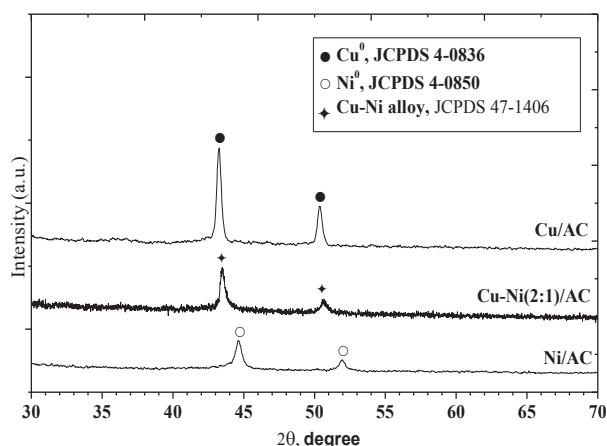


Figure 5 XRD of mono and bimetallic catalyst samples

Monometallic samples Cu/AC and Ni/AC display peaks corresponding to Cu⁰ [2θ = 43.3°, 50.4°, JCPDS file No. 4-0836 [37]] and Ni⁰ [2θ = 44.5°, 51.8°, JCPDS file No. 4-0850 [38]], respectively, indicating the formation of crystalline metal particles. Characteristic and well-defined diffraction peaks related to cubic phase Cu-Ni solid solution [2θ = 43.7°, 50.9°, JCPDS file No-47-1406] [39] for Cu:Ni molar ratio of 2:1 were observed in the bimetallic catalyst, indicating that Ni and Cu atoms were well mixed at atomic level [40], i.e., alloyed. Finally, the XRD patterns indicate the presence of metallic Cu, Ni and a cubic phase Cu-Ni alloy that were probably formed during reduction treatment. The crystallite sizes of copper, nickel and Cu-Ni alloy particles present in mono and bimetallic samples calculated with the Scherrer's equation are shown in Table 4. The estimated values for FWHM and θ_B were obtained from fitting the diffraction pattern at [111] plane with a Lorentzian function [30]. It is

observed that the crystallite size of bimetallic sample (23.9 nm) is closer to the size of Cu (23.5 nm) than to Ni (17.3 nm). On the other hand, particle size distribution was obtained from TEM of the powdered catalysts (not shown). Although the results may be different from the observed in the pellets, the comparison with crystallite size obtained by XRD of the pellets may be illustrative. In fact, although the average crystallite size of the bimetallic catalyst observed by TEM of the powdered catalysts (14.3 nm) is smaller than the value obtained from XRD of the pellets (23.9 nm), both techniques indicate that the crystallite size of the bimetallic catalysts is larger than the crystallite size of the Ni catalysts (10.8 and 17.3 nm from TEM and XRD, respectively). Therefore, the Cu would act as a "host" for Ni in the Cu-Ni solid solution. Indeed, a moderate antisegregation (i.e., Ni tends to stay in the bulk) has been reported for Cu-Ni alloys [41].

Table 4 Crystallite size of selected samples Cu, Ni and Cu-Ni/AC

Sample	θ _B (degree)	FWHM (degree)	Crystallite size (nm)
Cu/AC	43.25	0.38063	23.5
Ni/AC	44.63	0.52013	17.3
Cu-Ni(2:1)/AC	43.57	0.37325	23.9

Nitrogen adsorption/desorption isotherms for monometallic and Cu-Ni (2:1) catalysts, Figure 6, showed no significant changes with respect to AC support, indicating that catalysts retain the characteristic morphology of the support. Besides, the bimetallic catalyst displays a better adsorption capacity in agreement with its higher surface area compared to monometallic catalysts. All samples exhibited type IV isotherms with hysteresis loop type H4 according to IUPAC classification. These isotherms are usually found on mesoporous solids consisting of aggregated particles or agglomerates forming slit-shaped pores, with non-uniform size and shape [42]. The BHJ pore diameter distribution shows that all samples had narrow pore size distribution between 3 and 3.6 nm.

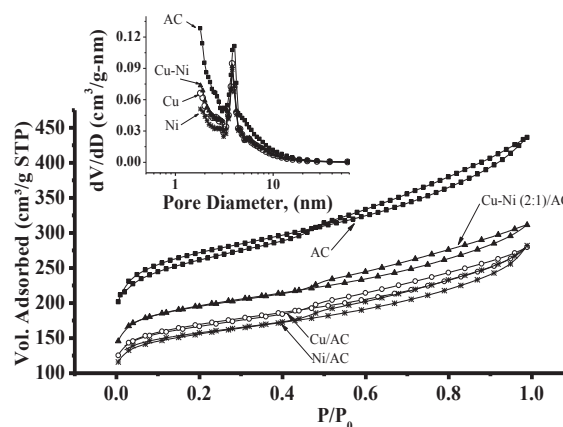


Figure 6 N₂ adsorption/desorption isotherms for AC support, monometallic and bimetallic samples. The insert corresponds to the BHJ pore diameter distribution

TPR profile of fresh Cu monometallic catalyst, Figure 7, displays a main reduction peak at 251°C and a weak shoulder at 290°C attributed to a two-step reduction of CuO to Cu₂O and Cu⁰ [43], respectively. TPR of Ni monometallic catalyst sample shows a main reduction peak at 281°C, and a smaller one at 380°C, both ascribed to reduction of NiO to Ni⁰ [44]. The shoulder at 242°C is attributed to the reduction of well-dispersed NiO particles on AC support [17]. An additional peak at 306°C, not found for the monometallic samples, was observed for the Cu-Ni(2:1)/AC sample. This points to the formation of Cu-Ni alloy species [45]. The broad peak observed after 500 °C, with a maximum at 600 °C, is associated with the partial gasification of carbon support due to CH₄ formation from the reaction of C and H₂ [46]; in fact, this peak is also present in the AC, indicating that the metals do not affect the high-temperature behavior of the support.

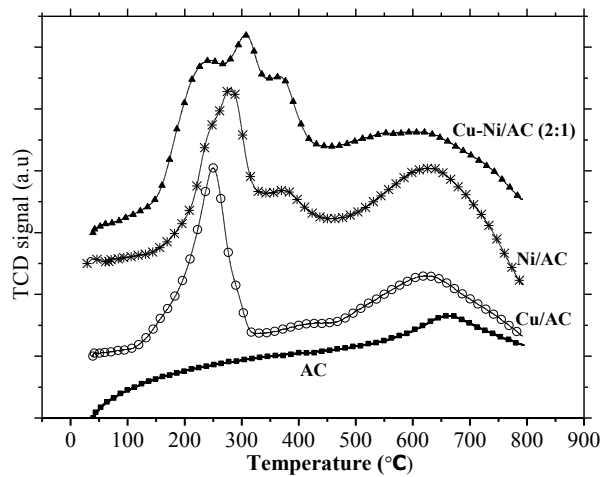


Figure 7 TPR profiles for activated carbon pellets AC, monometallic Cu/AC and Ni/AC and bimetallic Cu-Ni/AC 2:1 samples

Table 5 presents the consumption of H₂ in the TPR; the theoretical consumption was calculated from the actual metal loading (see Table 3) assuming a ratio of 1 mol H₂ per mol of metal oxide (i.e., CuO or NiO). Interestingly, despite its much lower amount in the catalysts (2.7 wt.% of Ni and 8.7 wt.% of Cu, see Table 3) the presence of Ni translates into an improved reducibility of the bimetallic catalyst.

Some typical SEM images are shown in Figure 8. From Figure 8(a) and Figure 8(b), it was possible to confirm the effective diameter of the pellets, 3.07 and 3.21 mm, respectively, values that are very close to the nominal size (3.175 mm). Figure 8(c) and Figure 8(d) confirm the presence of metal particles after the impregnation of activated carbon pellets. Specifically, energy dispersive X-ray analysis (not shown) suggests that white circular dots observed in Figure 8(d) correspond to clusters of metal particles of Cu and Ni with a surface chemical composition of 12.14% and 4.29%, respectively.

3.3. Catalytic activity

Effect of reaction temperature

Figure 9 shows the effect of reaction temperature on methanol conversion for pellets and powders under constant pressure (10 bar) and GHSV (988 h⁻¹); DMC selectivity of the pellets is also shown. An increase in the conversion of methanol is evidenced when catalyst is used in form of pellets instead of powder. This increase could be associated with the reduction in pressure drop in the reactor, which is close to 20% when powders are used in the bed.

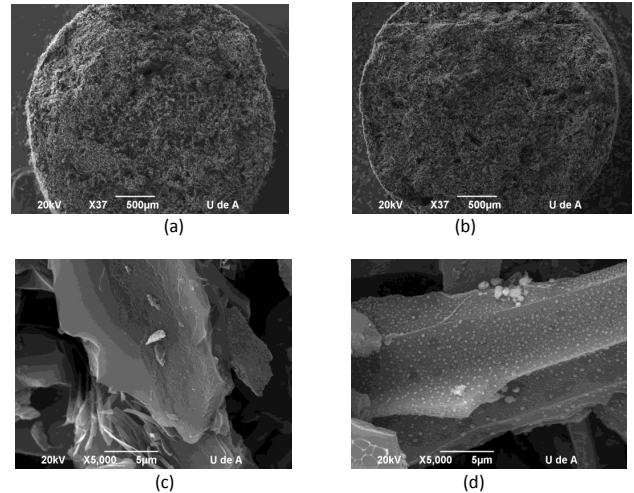


Figure 8 SEM images of (a) Ni/AC pellet; (b) Cu-Ni/AC 2:1 pellet; (c) AC x5000; (d) Cu-Ni/AC 2:1x5000

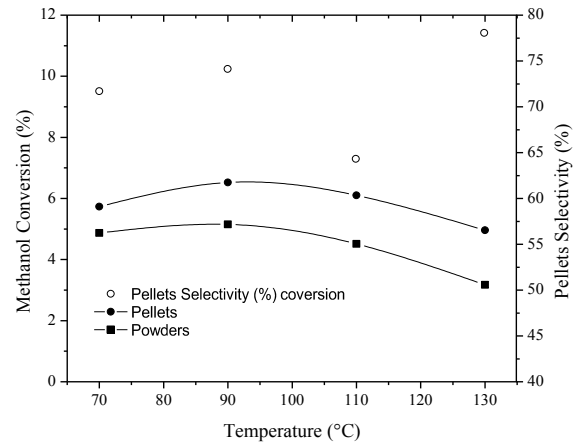


Figure 9 Effect of reaction temperature on methanol conversion (solid symbols) and DMC selectivity (open symbols) for pellets and powders. Catalyst weight: 1.7 g; P_{CO₂} = 10 bar; GHSV 988 h⁻¹

Methanol conversion appears to reach a maximum around 90°C with values of 6.52% and 5.15% for pellets and powder, respectively, and then decreases to 4.95% and 3.17%, respectively, as the temperature increases

Table 5 H₂ consumption and reducibility of the monometallic and bimetallic catalysts

Catalysts	Cu/AC	Ni/AC	Cu-Ni:2-1/AC
Theoretical consumption (mmol H ₂ /g cat)	2.03	1.61	1.84
Experimental consumption (mmol H ₂ /gcat)	0.29	0.34	0.4
Reducibility (%)	14.3	21.1	21.7

to 130°C; this trend would suggest a decrease of CO₂ adsorbed on the catalyst at high temperature. These trends are in agreement with those reported by [26], who showed an optimum temperature at 105°C using powdered bimetallic Cu-Ni/AC catalyst. Furthermore, previous studies of the gas-phase reaction over several materials [47-50] have been performed at temperatures from 40°C to 280°C, with optimum temperatures between 80°C and 130 °C. The simultaneous activation of methanol and CO₂ in this range of temperature would favor the formation of dimethyl carbonate over other products that would result from individual activation of the reactants. At lower temperatures, methanol conversions remain low, and at 110°C the selectivity towards DMC is drastically affected due to the tendency for methanol to form other reaction products such as HCHO, CO, methyl formate, dimethyl ether, dimethoxy methane, as well as the decomposition of DMC which increases over acidic catalysts [51].

Stability test

The catalytic performance was evaluated in terms of methanol conversion during 10 hours of reaction. The test was carried out at 130°C, 10 bar and a GHSV of 988 h⁻¹; the results are shown in Figure 10. Methanol conversion increases up to 2.5 h of reaction, and then slowly declines to a steady-state value at around 8%. The results obtained in this work are similar to powdered catalysts evaluated at 130°C and 10 bar which exhibited stable activity during 10 hours of reaction [26]; these conditions were selected to avoid partial condensation during the (long) test, according to a vapor-liquid equilibrium study previously reported [52]. Therefore, the pelletized catalyst is a promising material for DMC industrialization or application for new scale-up methodologies.

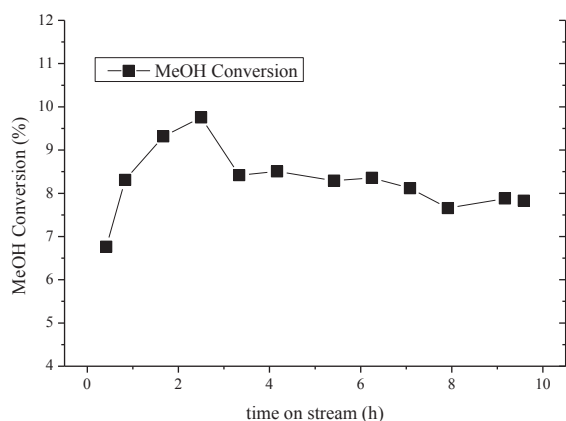


Figure 10 Stability test of catalyst pellets. Catalyst pellets weight: 1.7 g; T = 130°C; P = 10 bar, GHSV 988 h⁻¹

4. Conclusions

In this work, the effect of the addition of binder to activated carbon powders to form pellets that could be used as structured catalyst supports was analyzed. It was found that mixing activated carbon powders with CMC binder in 10% ethanol solution, using a carbon-binder ratio of 25 g AC/200 mL CMC_(sin) and treating the mixture by pyrolysis at 700 °C with a heating ramp of 20 °C/min, results in a low loss of surface area of obtained pellets; moreover, the loss of surface area is almost comparable to pyrolyzed powders indicating that during pyrolysis stage the CMC content is removed from the surface and pores of the carbon. Pellets obtained under these preparation conditions also showed good consistency, being more resistant to weight loss when they are subjected to vibration and rotation tests. Successful wet impregnation of Cu and Ni metals on pellets was developed using water as solvent for metal precursors. Catalysts characterization showed that formed pellets of Cu-Ni(2:1)/AC had higher surface area than monometallic samples (Cu/AC and Ni/AC), as well as the co-existence of Cu-Ni alloy species and metallic sites of Cu and Ni. In addition, the metal particles were well dispersed on the surface of carbon. Furthermore, bimetallic Cu-Ni catalyst supported on AC retains its activity when pelletized under favorable conditions which yield higher surface of samples. Moreover, pellets shown stability for 10 hours of reaction. All previous studies in the Cu-Ni bimetallic catalysts have been conducted in powder form; therefore, as a breakthrough in the application of the direct synthesis at a larger scale, the catalyst was successfully pelletized.

5. Acknowledgments

The financial support from Universidad de Antioquia through CODI Project Grant E01557 is gratefully acknowledged

6. References

1. N. Díez *et al.*, "A novel approach for the production of chemically activated carbon fibers", *Chem. Eng. J.*, vol. 260, pp. 463-468, 2015.
2. E. Gallegos, A. Guerrero, I. Rodriguez and A. Arcoya, "Comparative study of the hydrogenolysis of glycerol over Ru-based catalysts supported on activated carbon, graphite, carbon nanotubes and KL-zeolite", *Chem. Eng. J.*, vol. 262, pp. 326-333, 2015.
3. L. Pastor, R. Buitrago and A. Sepúlveda, "CeO₂-promoted Ni/activated carbon catalysts for the water-gas shift (WGS) reaction", *Int. J. Hydrogen Energy*, vol.

- 39, no. 31, pp. 17589-17599, 2014.
4. J. Zhao *et al.*, "Enhancement of Au/AC acetylene hydrochlorination catalyst activity and stability via nitrogen-modified activated carbon support", *Chem. Eng. J.*, vol. 262, pp. 1152-1160, 2015.
 5. D. Gudarzi, W. Ratchananusorn, I. Turunen, M. Heinonen and T. Salmi, "Promotional effects of Au in Pd-Au bimetallic catalysts supported on activated carbon cloth (ACC) for direct synthesis of H₂O₂ from H₂ and O₂", *Catal. Today.*, vol. 248, pp. 1-11, 2014.
 6. G. Zhang, A. Su, Y. Du, J. Qu and Y. Xu, "Catalytic performance of activated carbon supported cobalt catalyst for CO₂ reforming of CH₄", *J. Colloid Interface Sci.*, vol. 433, pp. 149-155, 2014.
 7. L. Xu *et al.*, "Catalytic CH₄ reforming with CO₂ over activated carbon based catalysts", *Appl. Catal. A Gen.*, vol. 469, pp. 387-397, 2014.
 8. T. Bao *et al.*, "Supported C₆₀O₄-C₆₀O₂ catalysts on modified activated carbon for CO preferential oxidation in H₂-rich gases", *Appl. Catal. B Environ.*, vol. 119, pp. 62-73, 2012.
 9. J. Bian *et al.*, "Direct synthesis of dimethyl carbonate over activated carbon supported Cu-based catalysts", *Chem. Eng. J.*, vol. 165, pp. 686-692, 2010.
 10. J. Bian *et al.*, "Highly effective synthesis of dimethyl carbonate from methanol and carbon dioxide using a novel copper-nickel/graphite bimetallic nanocomposite catalyst", *Chem. Eng. J.*, vol. 147, no. 2-3, pp. 287-296, 2009.
 11. J. Bian, M. Xiao, S. Wang, Y. Lu and Y. Meng, "Direct synthesis of DMC from CH₃OH and CO₂ over V-doped Cu-Ni/AC catalysts", *Catal. Commun.*, vol. 10, pp. 1142-1145, 2009.
 12. H. Xie, *et al.*, "Investigating the performance of CoxOy/activated carbon catalysts for ethyl acetate catalytic combustion", *Appl. Surf. Sci.*, vol. 326, pp. 119-123, 2015.
 13. O. Arbeláez, A. Orrego, F. Bustamante and A. Villa, "Direct Synthesis of Diethyl Carbonate from CO₂ and CH₃CH₂OH Over Cu-Ni/AC Catalyst", *Top. Catal.*, vol. 55, no. 7, pp. 668-672, 2012.
 14. P. Lazaridis *et al.*, "D-Glucose hydrogenation/hydrogenolysis reactions on noble metal (Ru, Pt)/activated carbon supported catalysts", *Catal. Today*, vol. 257, pp. 281-290, 2015.
 15. A. Al-Hassani, H. Abbas and W. Wan Daud, "Hydrogen production via decomposition of methane over activated carbons as catalysts: Full factorial design", *Int. J. Hydrogen Energy*, vol. 39, no. 13, pp. 7004-7014, 2014.
 16. E. Liakakou, E. Heracleous, K. Triantafyllidis and A. Lemonidou, "K-promoted NiMo catalysts supported on activated carbon for the hydrogenation reaction of CO to higher alcohols: Effect of support and active metal", *Appl. Catal. B Environ.*, vol. 165, pp. 296-305, 2015.
 17. E. Mostafavi, N. Mahinpey and V. Manovic, "A novel development of mixed catalyst-sorbent pellets for steam gasification of coal chars with in situ CO₂ capture", *Catal. Today*, vol. 237, pp. 111-117, 2014.
 18. A. Podgornik, A. Savnik, J. Jančar and N. Krajnc, "Design of monoliths through their mechanical properties", *J. Chromatogr. A.*, vol. 1333, pp. 9-17, 2014.
 19. Y. Matatov and M. Sheintuch, "Catalytic fibers and cloths", *Appl. Catal. A Gen.*, vol. 231, no. 1-2, pp. 1-16, 2002.
 20. C. Moreno and A. Pérez, "Carbon-Based Honeycomb Monoliths for Environmental Gas-Phase Applications", *Materials*, vol. 3, pp. 1203-1227, 2010.
 21. F. Rezaei and P. Webley, "Structured adsorbents in gas separation processes", *Sep. Purif. Technol.*, vol. 70, no. 3, pp. 243-256, 2010.
 22. D. Lozano, D. Cazorla, A. Linares and D. Quinn, "Activated carbon monoliths for methane storage: influence of binder", *Carbon*, vol. 40, pp. 2817-2825, 2002.
 23. K. Smith, G. Fowler, S. Pullket and N. Graham, "The production of attrition resistant, sewage-sludge derived, granular activated carbon", *Sep. Purif. Technol.*, vol. 98, pp. 240-248, 2012.
 24. A. Dashevsky, K. Kolter and R. Bodmeier, "Compression of pellets coated with various aqueous polymer dispersions", *Int. J. Pharm.*, vol. 279, pp. 19-26, 2004.
 25. F. Yu, L. Luo and G. Grevillot, "Adsorption Isotherms of VOCs onto an Activated Carbon Monolith: Experimental Measurement and Correlation with Different Models", *J. Chem. Eng. Data*, vol. 47, no. 3, pp. 467-473, 2002.
 26. J. Bian, M. Xiao, S. Wang, Y. Lu and Y. Meng, "Highly effective direct synthesis of DMC from CH₃OH and CO₂ using novel Cu-Ni/C bimetallic composite catalysts", *Chinese Chem. Lett.*, vol. 20, pp. 352-355, 2009.
 27. R. Saada, S. Kellici, T. Heil, D. Morgan and B. Saha, "Greener Synthesis of Dimethyl Carbonate using a Novel Ceria-Zirconia Oxide/Graphene Nanocomposite Catalyst", *Appl. Catal. B Environ.*, vol. 168, pp. 353-362, 2014.
 28. J. Wang, W. Zhu, S. Yang, W. Wang and Y. Zhou, "Catalytic wet air oxidation of phenol with pelletized ruthenium catalysts", *Appl. Catal. B Environ.*, vol. 78, pp. 30-37, 2008.
 29. G. Leofanti *et al.*, "Catalyst characterization: characterization techniques", *Catal. Today*, vol. 34, pp. 307-327, 1997.
 30. A. Mikrajuddin and K. Khairurrijal, "Derivation of Scherrer Relation Using an Approach in Basic Physics Course", *J. Nanosains*, vol. 1, pp. 28-32, 2008.
 31. C. Li and S. Zhong, "Study on application of membrane reactor in direct synthesis DMC from CO₂ and CH₃OH over Cu-KF/MgSiO catalyst", *Cat. Today*, vol. 82, pp. 83-90, 2003.
 32. K. Almusaitee, "Synthesis of dimethyl carbonate (DMC) from methanol and CO₂ over Rh-supported catalysts", *Catal. Comm.*, vol. 10, pp. 1127-1131, 2009.
 33. D. de Britto and O. Assis, "Thermal degradation of carboxymethylcellulose in different salty forms", *Thermochimica Acta*, vol. 494, pp. 115-122, 2009.
 34. P. Webb and C. Orr, *Analytical methods in fine particle technology*, 1st ed. Norcross, USA: Micromeritics Instrument Corporation, 1997.
 35. F. Delannay, *Characterization of Heterogeneous Catalysts*, 1st ed. New York, USA: Marcel Dekker, Inc., 1984.
 36. J. Bian, M. Xiao, S. Wang, Y. Lu and Y. Meng, "Highly effective direct synthesis of DMC from CH₃OH and CO₂ using novel Cu-Ni/C bimetallic nanocomposite catalysts", *Chin. Chem. Lett.*, vol. 20, no. 3, pp. 352-355, 2009.
 37. T. Theivasanthi and M. Alagar, "Nano sized

- copper particles by electrolytic synthesis and characterizations", *Int. J. Physical Sci.*, vol. 6, pp. 3662-3671, 2011.
38. J. Ashok and S. Kawi, "Steam reforming of toluene as a biomass tar model compound over CeO₂ promoted Ni/CaO-Al₂O₃ catalytic systems", *Int. J. Hydrogen Energy*, vol. 38, no. 32, pp. 13938-13949, 2013.
 39. I. Baskaran, T. Sankara and A. Stephen, "Pulsed electrodeposition of nanocrystalline Cu-Ni alloy films and evaluation of their characteristic properties", *Mater. Lett.*, vol. 60, no. 16, pp. 1990-1995, 2006.
 40. C. Jung, H. Lee, C. Kim and S. Bhaduri, "Synthesis of Cu-Ni alloy powder directly from metal salts solution", *J. Nanopart. Res.*, vol. 5, pp. 383-388, 2003.
 41. B. Hammer and J. Nørskov, "Theoretical Surface Science and Catalysis—Calculations and Concepts", *Advances in Catalysis*, vol. 45, pp. 71-129, 2000.
 42. G. Leofanti, M. Padovan, G. Tozzola and B. Venturelli, "Surface area and pore texture of catalysts", *Catal. Today*, vol. 41, pp. 207-219, 1998.
 43. C. Chen, J. Lin, T. Lai and B. Li, "Active sites on Cu/SiO₂ prepared using the atomic layer epitaxy technique for a low-temperature water-gas shift reaction", *J. Catal.*, vol. 263, pp. 155-166, 2009.
 44. M. Cangiano, M. Ojeda, A. Carreras, J. González and M. Ruiz, "A study of the composition and microstructure of nanodispersed Cu-Ni alloys obtained by different routes from copper and nickel oxides", *Mater. Charact.*, vol. 61, pp. 1135-1146, 2010.
 45. O. Ilinich, W. Ruettinger, X. Liu and R. Farrauto, "Cu-Al₂O₃-CuAl₂O₄ water-gas shift catalyst for hydrogen production in fuel cell applications: Mechanism of deactivation under start-stop operating conditions", *J. Catal.*, vol. 247, pp. 112-118, 2007.
 46. X. Zhang, Y. Zhang, Q. Liu and W. Zhou, "Surface properties of activated carbon from different raw materials", *Int. J. Min. Sci. Technol.*, vol. 22, pp. 483-486, 2012.
 47. J. Bian, M. Xiao, S. Wang, Y. Lu and Y. Meng, "Carbon nanotubes supported Cu-Ni bimetallic catalysts and their properties for the direct synthesis of dimethyl carbonate from methanol and carbon dioxide", *Appl. Surf. Sci.*, vol. 255, no. 16, pp. 7188-7196, 2009.
 48. X. Wu, M. Xiao, Y. Meng and Y. Lu, "Direct synthesis of dimethyl carbonate on H₃PO₄ modified V₂O₅", *J. Mol. Catal. A Chem.*, vol. 238, pp. 158-162, 2005.
 49. A. Aouissi, A. Apblett, Z. AL-Othman and A. Al-Amro, "Direct synthesis of dimethyl carbonate from methanol and carbon dioxide using heteropolyoxometalates: the effects of cation and addenda atoms", *Transit. Met. Chem.*, vol. 35, pp. 927-931, 2010.
 50. X. Wu, Y. Meng, M. Xiao and Y. Lu, "Direct synthesis of dimethyl carbonate (DMC) using Cu-Ni/VSO as catalyst", *J. Mol. Catal. A Chem.*, vol. 249, pp. 93-97, 2006.
 51. J. Zawadzki, B. Azambre, O. Heintz, A. Krztoń and J. Weber, "IR study of the adsorption and decomposition of methanol on carbon surfaces and carbon-supported catalysts", *Carbon*, vol. 38, no. 4, pp. 509-515, 2000.
 52. F. Bustamante, A. Orrego, S. Villegas and A. Villa, "Modeling of Chemical Equilibrium and Gas Phase Behavior for the Direct Synthesis of Dimethyl Carbonate from CO₂ and Methanol", *Industrial & Engineering Chemistry Research*, vol. 51, pp. 8945-8956, 2012.